Poly(lactic acid)-hyperbranched polyglycerol nanoparticles enhance bioadhesive treatment of esophageal disease and reduce systemic drug exposure

Yang Mai[1†], Yaqi Ouyang[1†], Yujia Qin[1], Changchang Jia[2], Laura E. McCoubrey[3], Abdul W. Basit[3], Yichu Nie[4], Yizhen Jia[1], Liu Yu[1], Liu Dou[1], Wenbin Deng[1], Yang Deng[1]*, Yang Liu[1]*

[1] School of Pharmaceutical Sciences (Shenzhen), Sun Yat-sen University, Guangzhou, 510275, China

[2] Cell-Gene Therapy Translational Medicine Research Center, The Third Affiliated Hospital of Sun Yat-sen University, Guangzhou, 510000, China

[3] UCL School of Pharmacy, University College London, 29–39 Brunswick Square, London WC1N 1AX, UK

[4] Clinical Research Institute, The First People's Hospital of Foshan & Sun Yat-sen University Foshan Hospital, Foshan, 528000, China

† These authors contributed equally to this work.

* Correspondence: dengy67@mail.sysu.edu.cn; liuyang65@mail.sysu.edu.cn

Abstract

The effective treatment of esophageal disease represents a significant unmet clinical need, as existing treatments often lead to unnecessary systemic drug exposure and suboptimal concentrations at the disease site. Here, surface-modified bioadhesive poly(lactic acid)-hyperbranched polyglycerol nanoparticles (BNPs), with an average 100 - 200 nm diameter, were developed for local and sustained esophageal drug delivery. BNPs showed significantly higher adhesion and permeation into *ex vivo* human and rat esophageal tissue than non-adhesive nanoparticles (NNPs) and had longer residence times within the rat esophagus *in vivo*. Incubation with human esophagus (Het-1A) cells confirmed BNPs' biocompatibility at clinically relevant concentrations. In a rat model of achalasia, nifedipine-loaded BNPs significantly enhanced esophageal drug exposure, increased therapeutic efficacy, and reduced systemic drug exposure compared to NNPs and free drug. The safety of BNPs was demonstrated by an absence of intestinal, hepatic, and splenic toxicity following administration. This study is the first to demonstrate the efficacy of BNPs for esophageal drug delivery and highlight their potential for improving the lives of patients suffering with esophageal conditions.

Keywords

Local drug delivery; co-polymer synthesis; surface-modified nanoparticles; oesophageal disease; chronic disease treatment; formulation optimization.

1. Introduction

Esophageal diseases affect millions of patients worldwide. In 2021 there were an estimated 19,260 new cases of esophageal cancer in the United States (U.S.) alone [1]. Based on previous data, these patients have just a 19.9% relative survival rate over the following 5 years, with the disease regarded as one of the world's most lethal cancers [2]. Like esophageal cancer, many local diseases of the esophagus carry debilitating symptoms, poor cure rates, and substantial economic burden. For example, achalasia, an esophageal motor disorder involving insufficient relaxation of the lower esophageal sphincter (LES), is currently regarded as incurable and accounts for over $400 million direct medical costs in the U.S. annually [3]. Moreover, chronic diseases such as eosinophilic esophagitis and gastroesophageal reflux disease (GERD) are increasing in prevalence and collectively affect millions of people worldwide each year [4, 5]. Though the esophagus is a reasonably accessible body site, medications intended to manage and treat esophageal conditions are typically not designed to exert their therapeutic action locally; instead drugs are delivered systemically for eventual permeation of esophageal tissues via the circulation. These untargeted formulations do not optimise esophageal drug concentrations and frequently result in adverse effects due to systemic exposure. For instance, there has been no profound clinical benefit gained from developments in esophageal cancer treatment for 30 years, with existing chemotherapeutics commonly injected causing significant toxicity to the immune and gastrointestinal systems [2].

Patients suffering from esophageal diseases are in great need of new treatments with enhanced efficacy and lower incidence of adverse events. To achieve this, delivering drugs directly to esophageal tissue is a promising strategy as local drug concentrations will be optimised whilst systemic drug exposure is limited [6]. Though conceptually simple, this strategy does comprise several challenges that are innate to the esophageal environment and its associated pathologies. Firstly, the typical transit time of the esophagus is just 10 seconds, therefore targeted formulations will likely require increased local residence times in order to deliver drugs to surrounding tissues [7].

Secondly, the esophagus has an unstirred water layer of around 30 μm which therapeutics will need to cross to reach underlying mucosal cells [8]. To avoid solubilized drugs being washed into the stomach before they can reach the esophageal epithelium, formulations may need reliable bioadhesive properties to deliver drug molecules directly to the mucosa [6]. Finally, esophageal blockage is a key concern for patients with esophageal disease. Many esophageal diseases can cause strictures, a condition in which the esophageal lumen is narrowed, for example due to tumor invasion, inflammation, or tissue damage [9]. Accordingly, treatments targeted to the esophagus should be mindful of the underlying pathology and avoid increasing the risk of esophageal blockage at all costs. For this reason, large solid dosage forms may be less suitable for patients at risk of esophageal strictures [10, 11]. Whilst stents are often offered to patients with strictures, whereby the esophageal lumen is opened using a tube or scaffold [12-14], these interventions are invasive and commonly cause complications, such as recurrent dysphagia, pain, and infection [15, 16]. Consequently, non-invasive treatments for esophageal disease are highly sought.

Formulations incorporating increased esophageal residence time, mucosal adhesion, and minimal risk of luminal blockage could come in a variety of forms. Liquid dosage forms have been especially researched for esophageal drug delivery [17-19]. For example, alginate solutions have demonstrated moderate adhesion to *ex vivo* esophageal mucosa, with 20% of doses associated with tissue after 30 minutes of washing [20]. Elsewhere, a chitosan-based hydrogel loaded with hexylaminolevulinate demonstrated a residence time of 10 min, sufficient for the diagnosis of Barrett's esophagus in patients [21]. In comparison, a solid oral dosage form based on chitosan granules dispensed in gelatin capsules achieved > 66% retention in the human esophagus for 1.75 h [22]. Despite these positive steps, there still remains an opportunity for formulations that can prolong drug residence time in the esophagus. In this study, we produced bioadhesive nanoparticles (BNPs) by oxidizing vicinal diols on the surface of nonadhesive nanoparticles (NNPs) into aldehydes (Figure 1a). Exposed aldehyde moieties on the surface of BNPs allow them to adhere to protein-rich

substances by forming covalent Schiff-base bonds with amine groups in amino acids. The starting NNPs were formulated from polylactic acid block–hyperbranched polyglycerol (PLA-HPG) co-polymers due to their low immunogenicity, stability against aggregation, and diffusive properties [23]. Also, these biodegradable synthetic polymers, such as PLA, have tailorable porosity and degradation time which are advantageous drug carriers [24, 25]. In previous studies, these BNPs have been formulated into sunscreen to achieve enhanced skin adhesion [26] and have successfully reduced systemic toxicity whilst improving retention of chemotherapeutics after intraperitoneal and intratumoral administration [27, 28]. In this work, we translated the BNP technology for treatment of esophageal disease by utilising a rat model of achalasia. Nifedipine was selected as a model drug to be delivered by BNPs, as it has demonstrated clinical efficacy in achalasia however is not currently recommended due to its significant systemic side effects [29]. We aimed to prove that BNPs could better adhere to the esophageal mucosa, prolong esophageal drug retention, and limit systemic drug exposure compared to NNPs (Figure 1b).

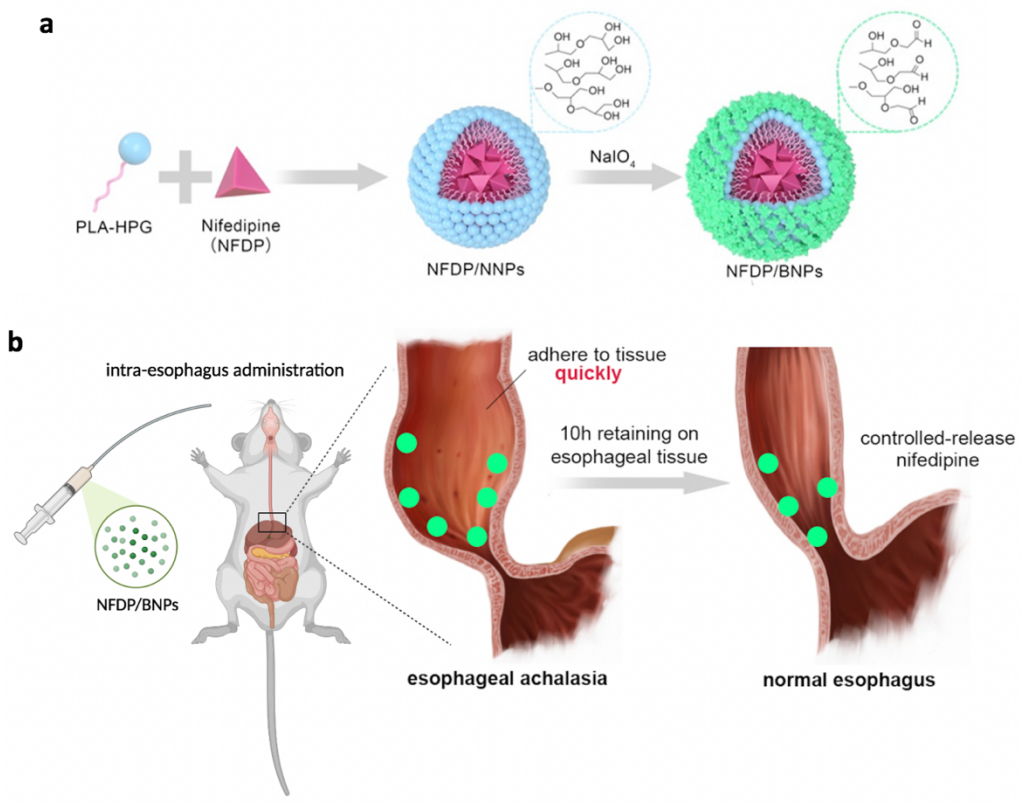

Figure 1. Schematic illustration of the preparation of nifedipine-loaded

nanoparticles (NPs). a) Nifedipine (NFDP)/NNPs were prepared through NFDP and PLA-HPG self-assembly. NFDP/NNPs could be further converted into NFDP/BNPs after NaIO4 treatment of vicinal diols on the surface of NNPs. b) NFDP/BNPs would retain on the esophageal mucosa over 10 h and controlled release NFDP.

2. Results and discussion

2.1 Characterization and *in vitro* evaluation of NPs

Dynamic light scattering demonstrated that BNPs (with and without NFDP loading) could be synthesised from NNPs without significant changes to hydrodynamic size (Figure 2a). 100 - 200 nm was considered as an optimum diameter for diffusion into esophageal tissue [30]. Further, the uniformity and spherical structure of NPs was confirmed using TEM (Figure 2b). The results demonstrate that NFDP encapsulation and the oxidative conversion of NNPs to BNPs did not significantly alter their particle sizes or morphologies (Figures 2a and b). PLA-Cy5/NNPs and PLA-Cy5/BNPs showed comparable diameters to NFDP/NNPs and NFDP/BNPs (Supplementary Figure 2a).

Though intended for esophageal action only, NPs may transit through the whole digestive tract if they do not fully adhere to the esophageal wall. Therefore, the *in vitro* toxicity of NPs was measured using Het-1A and Caco-2 cells at a range of concentrations (Figure 2c). All NPs (NNPs, BNPs, NFDP/NNPs and NFDP/BNPs) at concentrations of 0.001 mg/mL to 5 mg/mL showed no significant impact on cell viability of both cell lines compared with untreated controls. These results demonstrated that the NPs were safe to progress to subsequent *in vivo* studies.

When examining NPs' adhesion to poly-L-lysine (a model peptide), NFDP/BNPs were recovered at a rate of approximate 15%, while NFDP/NNPs showed an extremely low recovery rate (Figure 2d), demonstrating the enhanced bioadhesion of BNPs. The data highlights that NFDP encapsulation into BNPs did not prevent adhesion of the NP

surface aldehyde groups to amino acids. Whilst peptide adhesion of NFDP/BNPs was significantly ($p < 0.001$) higher than achieved by NFDP/NNPs, the *in vitro* drug release assessment showed that NFDP/NNPs and NFDP/BNPs exhibited similar release profiles (Figure 2e).

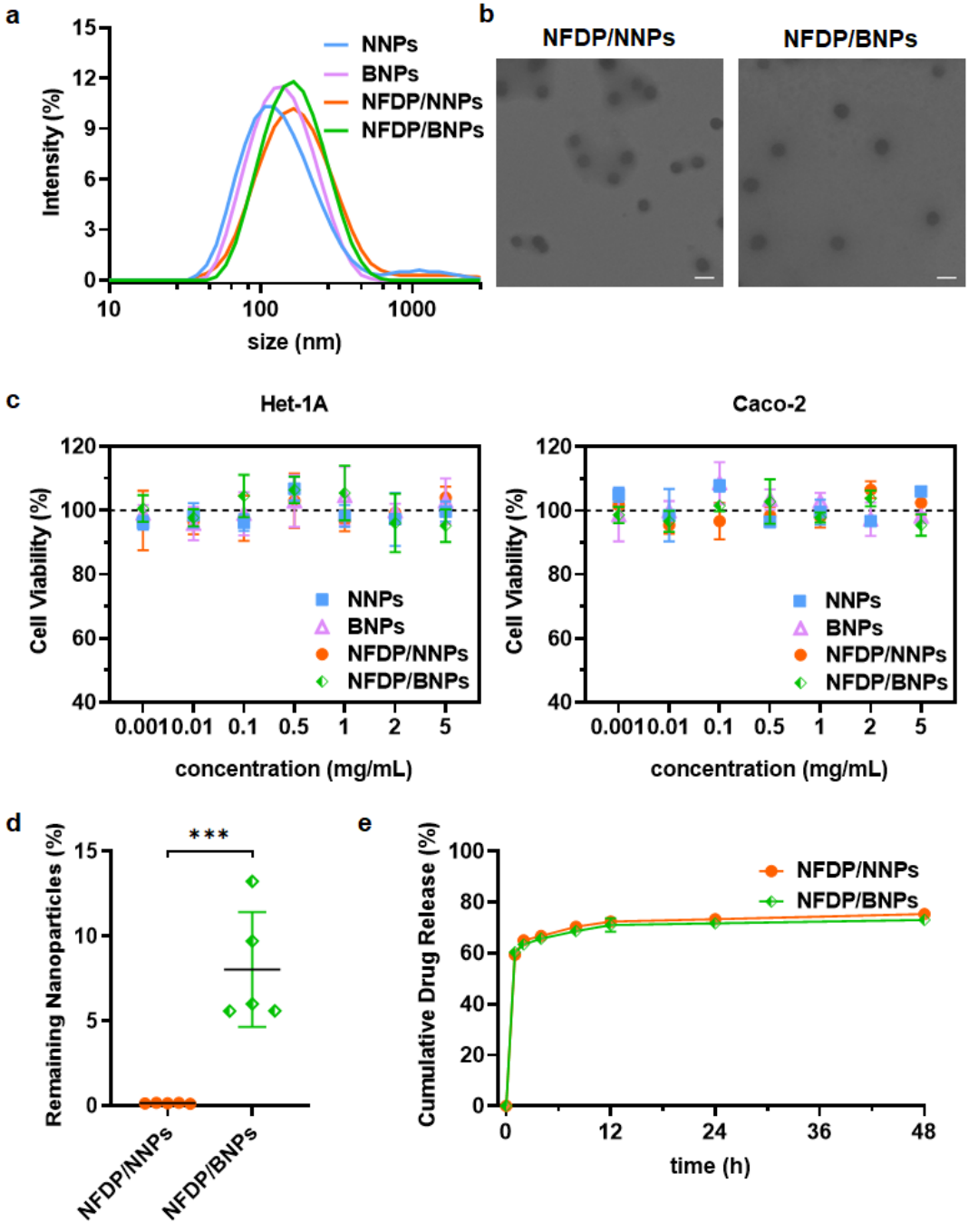

Figure 2. Characterization and *in vitro* evaluation of NPs. a) Hydrodynamic diameter distribution of blank NNPs, BNPs, NFDP/NNPs and NFDP/BNPs by dynamic

light scattering. b) Transmission electron microscopy (TEM) images of NFDP/NNPs and NFDP/BNPs. Scale bar on images represents 200 nm. c) Cell viability of cultured human esophagus (Het-1A) and human colorectal adenocarcinoma cell (Caco-2) treated with blank NNPs, BNPs, NFDP/NNPs and NFDP/BNPs at various concentrations (n = 5). d) The recovery rate of drug-loaded NPs after rinsing on a poly-L-lysine-coated 96-well-plate. Results were normalized to the average absorbance intensity of drug-loaded NPs before rinsing (n = 5). e) *In vitro* release profile of NFDP from NFDP/NNPs or NFDP/BNPs in PBS (n = 5).

2.2 BNPs improve *ex vivo* bioadhesion and tissue permeation

The *ex vivo* adhesion and permeation of BNPs and NNPs was assessed by applying Cy5 dye conjugated NPs onto the surface of human and rat esophageal tissues (Figure 3a and Supplementary Figure 4a). Almost no Cy5-PLA released from NNPs or BNPs over 24 h, with ~ 99% of dye remaining in both NNPs and BNPs even after 48 h (Supplementary Figure 2b), indicating the accuracy of quantification of NPs based on Cy5 fluorescence levels. After 15 s incubation on the mucus surface of rat esophageal tissue, followed by continuous saline irrigation for 30 s, the retention of BNPs was significantly higher than that of NNPs (Figures 3b-c). More interestingly, the bioadhesion of BNPs to esophageal tissue was not affected by simulated gastric fluid (Supplementary Figure 3), which supported the bioadhesiveness of BNPs in acid microenvironment caused by related diseases, such as acid reflux. Further inspection of the tissue found that BNPs diffused across the mucus into the esophageal tissue, whilst NNPs did not (Figures 3d-e). These results suggest that BNPs could adhere to tissue in ≤ 15 s, withstanding saline rinsing designed to mimic saliva flow and fluid intake.

Using esophageal tissues from human volunteers, it was again observed that BNPs adhered to the epithelial surface better than NNPs (Supplementary Figure 4). Specifically, 50% of BNPs were retained on the human esophageal epithelium compared to < 5% of the NNPs (Supplementary Figures 4b-c). Further, BNPs were observed to diffuse deeper into human esophageal tissues than NNPs (Supplementary

Figures 4d-e). Ideal formulations for esophageal delivery should quickly attach to the esophagus and improve drug permeation into esophageal tissue. These results confirm the bioadhesion of BNPs and their permeation into human esophageal tissue for the first time, highlighting their potential as targeted drug delivery agents for treatment of local disease. A liquid formulation was selected as an alternative to a solid dosage form due to patients' higher risk of developing esophageal strictures and dysphagia [31]. These results demonstrate that the liquid formulation adequately delivered BNPs, allowing their adhesion and permeation into *ex vivo* esophageal tissue.

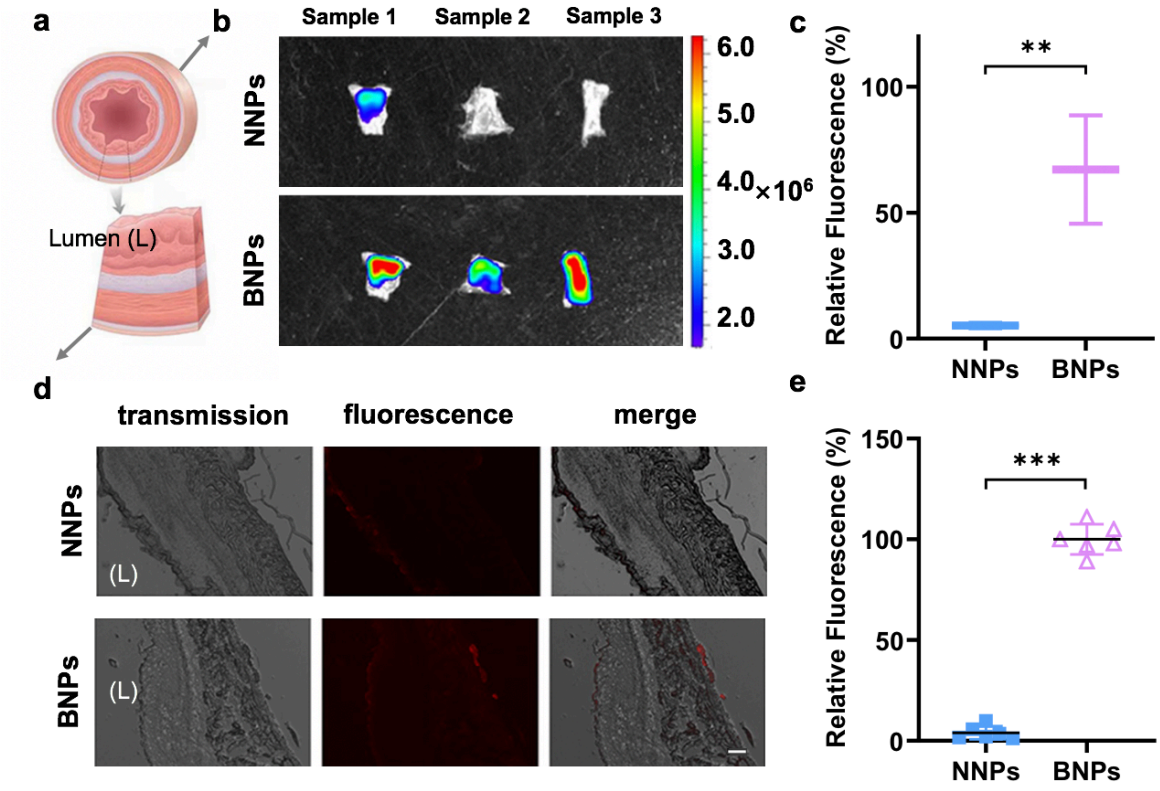

Figure 3. *Ex vivo* evaluation of NPs adhesion and diffusion on rat esophagus tissues. a) A diagram of esophageal tissues used and imaged in this study. b) NNPs and BNPs encapsulating PLA-Cy5 dye were added on the surface of esophageal tissues from rats for 15 s. *Ex vivo* tissue images were taken with Xenogen after 30s saline rinsing. c) The remaining fluorescence intensity of NNPs and BNPs on esophagus tissues was quantified and normalized to the average fluorescence of NPs before saline rinsing. Data are shown as mean ± s.d. (n = 3). d) NNPs and BNPs encapsulating PLA-Cy5 dye

were added on the surface of esophageal tissues from rats for 15 s following by 1 h incubation at 37 °C. Frozen sections were collected and imaged with fluorescence microscope. Left column, transmission channel; middle column, Cy5 fluorescence channel, Cy5 signal in red; right column, merge images of left and middle columns. (L) indicated as lumen side of the esophagus tissues. Scale bars, 100 μm (applies to all images). e) The fluorescence of images from **d** was quantified and normalized to the average fluorescence of BNPs treated samples. Data are shown as mean ± s.d. (n = 6). Asterisks indicate: $p < 0.01$ (**) and $p < 0.001$ (***).

2.3 BNPs enhance the *in vivo* esophageal retention of NPs

After intra-esophageal administration NPs were mostly retained at rats' lower esophagus, especially around the LES (Figure 4a). BNPs showed statistically faster and enhanced adhesion to the esophagus compared to NNPs. The esophageal retention efficiency of NNPs was 75% lower than that achieved by the BNPs at 6 min after administration (Figure 4b). Almost no NNPs were found on esophageal tissue at 2 h post treatment while BNPs showed over 73% retention: 15-fold higher than that of NNPs. After 10 h, BNPs exhibited over 30% retention and were present up to 24 h post treatment (Figure 4c). In comparison, no NNPs were found in the esophagus after 10 h. This residence time is far better than that achieved by the best-performing dosage form found in the literature (capsules with retentions of 1.75 h) [22]. Figure 3d shows that at 10 h post treatment the samples treated with BNPs showed widespread NP distribution and diffusion.

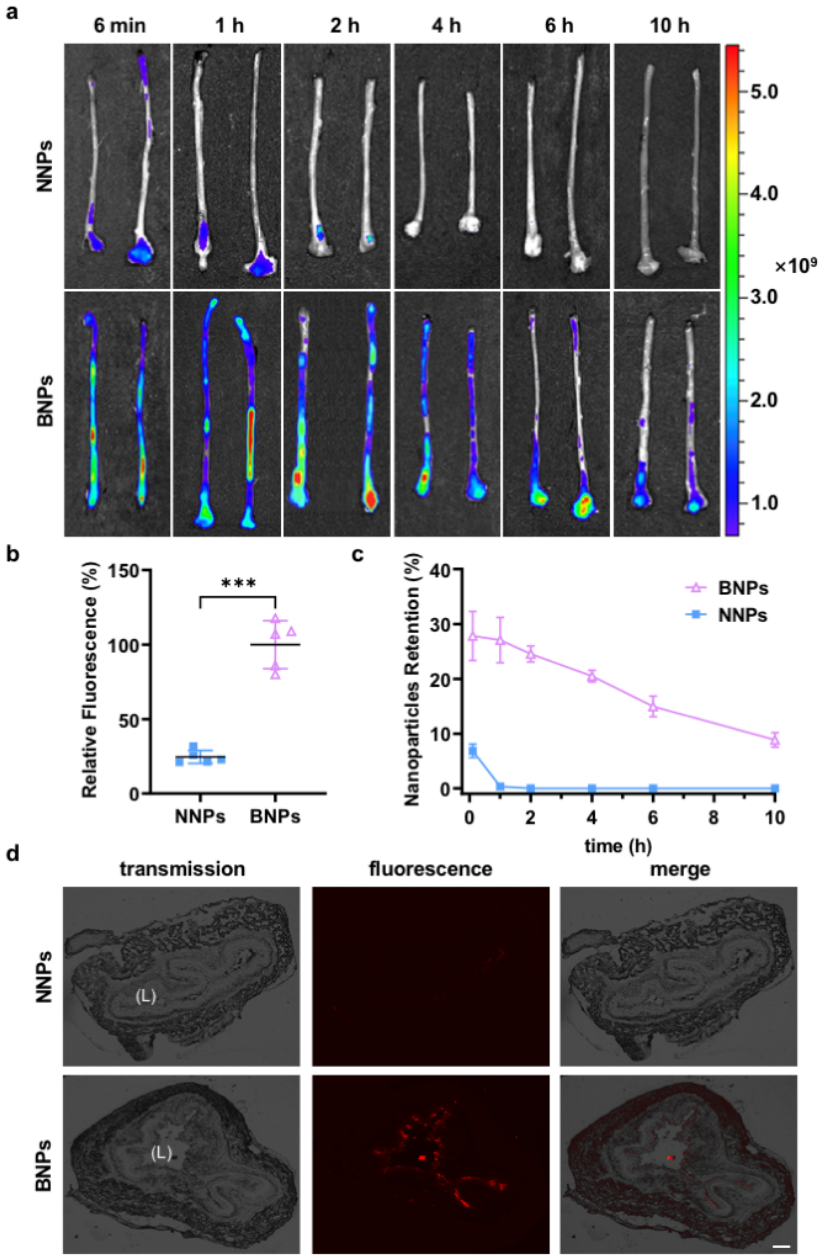

214

215 **Figure 4. *In vivo* evaluation of esophageal retention and diffusion of NPs.** a) NNPs
216 and BNPs encapsulating PLA-Cy5 dye were intra-esophageally administrated to the
217 rats. *Ex vivo* images of esophagus retention were taken with Xenogen at different time
218 points after administration. b) The fluorescence intensity of esophageal tissue after
219 treatment with NNPs or BNPs was quantified and normalized to the average
220 fluorescence of BNPs treatment at 6 min post-administration (n = 5). c) The
221 fluorescence intensity of esophageal tissue at different timepoints following exposure
222 to NNPs or BNPs was quantified and normalized to the initial fluorescence intensity of

tissue before administration (n = 4). c) Representative frozen sections of esophageal tissue from NNPs or BNPs treated groups at 10 h post treatment. Left column, transmission channel; middle column, Cy5 fluorescence channel, Cy5 signal in red; right column, merge images of left and middle columns. (L) indicated as lumen side of the esophagus tissues. Scale bars, 100 μm (applies to all images).

2.4 BNPs enhance the *in vivo* esophageal retention of nifedipine (NFDP)

At 6 minutes after administration, NFDP/BNPs delivered 32% of their drug dose to the rat esophagus compared to < 8% and 1% for the NFDP/NNPs and free NFDP, respectively (Figure 5a). BNPs' esophageal adhesion was significantly enhanced over that of free NFDP and NFDP/NNPs. NFDP delivered with NNPs or as a free drug solution was hardly found on esophageal tissue after 1 h, compared to 27% of the initial NFDP dose achieved by NFDP/BNPs. At 10 h approximately 10% of the initial NFDP dose was still present in the esophagus following BNP administration, the same concentration remaining at 6 min following administration of NFDP/NNPs. Thus, BNPs encapsulation substantially prolonged NFDP retention in the esophagus compared with encapsulation in NNPs or as free drug, suggesting that BNPs could enable site-specific drug delivery to esophageal tissue. This could reduce systemic drug exposure and improve therapeutic efficacy due to increased drug concentrations at the disease site. As 70% NFDP was released from BNPs over 10 h during *in vitro* studies (Figure 2e), it is likely that NFDP could be released from BNPs and exert its therapeutic action *in vivo* during the time BNPs remain resident in the esophagus.

Results regarding systemic bioavailability of NFDP supported the potential of BNPs. Much lower NFDP bioavailability was observed when delivering NFDP/BNPs compared with free NFDP and NFDP/NNPs ($p < 0.05$), demonstrating NFDP released from BNPs mainly localized on the esophageal tissue instead of being absorbed and distributed throughout the whole body (Figure 5b). Previous work based on local action of nitrites within the esophagus showed that fewer side effects occur with local drug delivery compared to systemic administration [32]. These findings support the

conclusion that BNPs are likely to reduce systemic drug side effects by targeting drugs directly to their site of action in the esophagus.

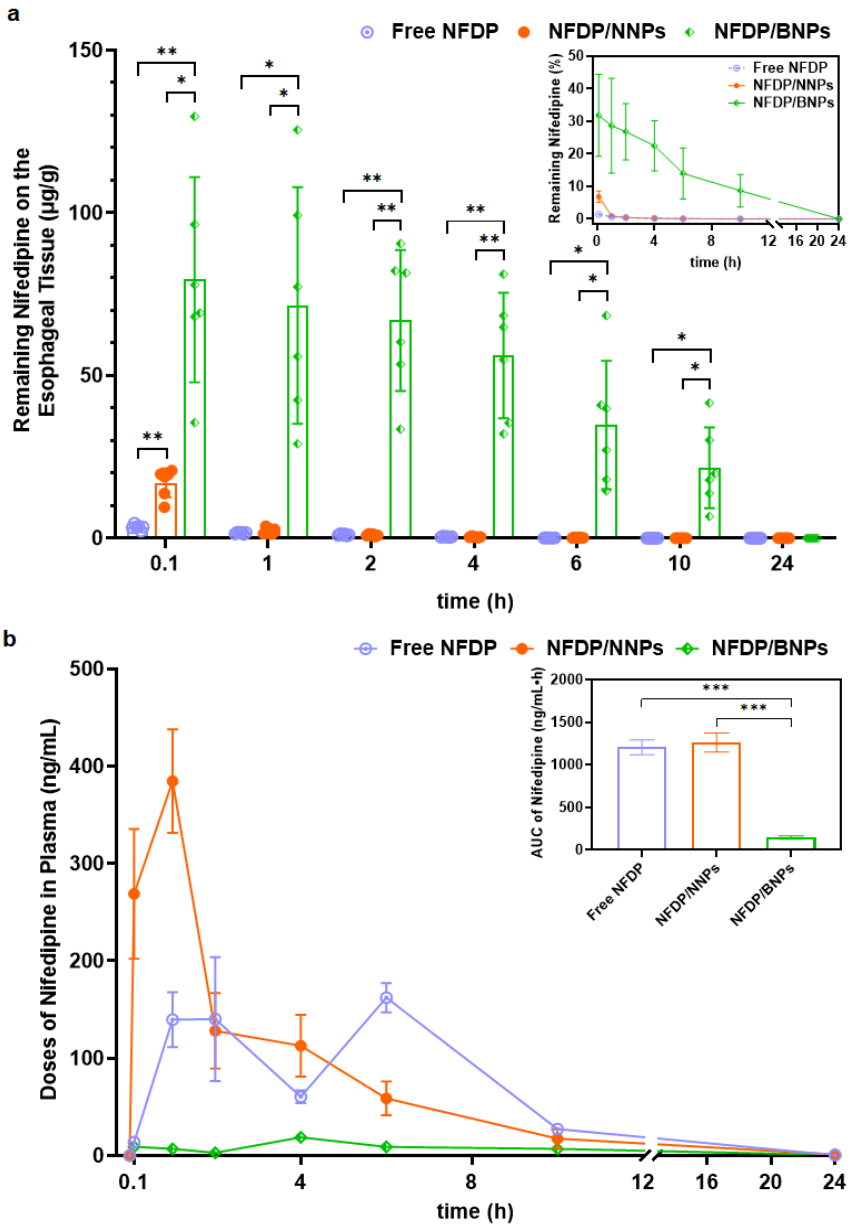

Figure 5. Accumulation of NFDP in the esophagus and plasma of achalasia rats following administration of free NFDP (nifedipine), NFDP/NNPs, and NFDP/BNPs. a) The concentration of NFDP remaining in rats' esophageal tissues for 24 hours after administration of free NFDP, NFDP/NNPs, and NFDP/BNPs. b) The

concentration of NFDP in rats' plasma for 24 hours after administration of free NFDP, NFDP/NNPs, and NFDP/BNPs. n = 5 rats were studied at each timepoint.

2.5 BNPs enhance the therapeutic efficacy of NFDP in rat models of achalasia

The rat model of achalasia was successfully produced by injecting 0.2% BAC into the abdominal portion of the esophagus for ablation of the ganglion cells of the myenteric plexus [33]. Pathological changes were observed mainly in the middle and lower thirds of the esophagus, resulting in reductions in body weight and food intake, malnutrition and immune impairment. The animal model set up and treatment plan are summarized in Figure 6a. The body weights of diseased rats decreased continuously during the 21-day pre-treatment period (Figure 6b), and megaesophagus was confirmed in the radiographic study after the disease models were successfully set-up (Figure 6c). Treatments were subsequently administered once daily for 7 days (Figure 6a), and within 3 days the body weights of achalasia rats treated with NFDP/BNPs increased in the same trend as healthy untreated rats and the sham-operated group, whilst treatment with free NFDP and NFDP/NNPs showed no significant influences on body weight compared to the saline treated rats (Figure 6d and Supplementary Figure 5a). Between treatment days 4 to 7 diseased rats administered NFDP/BNPs showed a significantly larger increase in body weight compared with that of free NFDP and NFDP/NNPs. The food intake for each rat was also recorded, and a similar trend was observed (Figure 6e and Supplementary Figure 5b). In this regard, achalasia rats ingested significantly more food during treatment with NFDP/BNPs compared to those treated with free NFDP, NFDP/NNPs or the saline-administered diseased controls. Favorably, rats treated with NFDP/BNPs had comparable food intake to the healthy and sham-operated rats. As demonstrated in Figure 4a BNPs provided a sustained release of NFDP within the rat esophagus, which is likely to continuously relax the LES, improve esophageal emptying, and thus enhance therapeutic efficacy. The safety profile of NFDP/BNPs was also positive, as no *in vivo* toxicity was found in the stomachs, intestines, livers or spleens of rats after any treatments (Supplementary Figure 6). These findings are

supported by that presented in Figure 6b, in which systemic drug exposure from NFDP/BNPs was much lower than that observed from free NFDP or NFDP/NNPs. Overall, the results shown here highlight NFDP/BNPs as a safe and effective therapy for achalasia with significant benefits over untargeted free drug and NPs lacking bioadhesive properties.

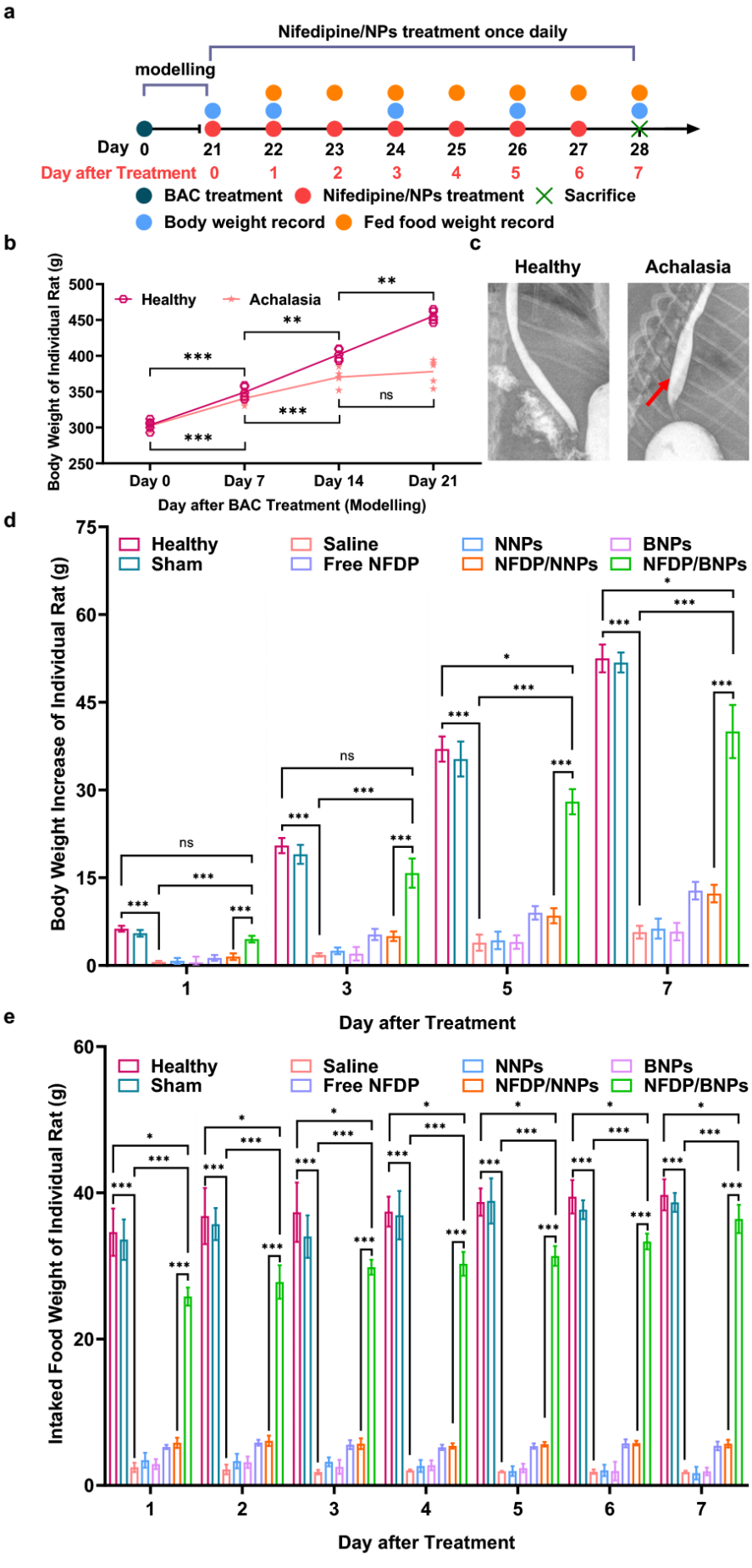
a
Nifedipine/NPs treatment once daily
modelling
Day 0 21 22 23 24 25 26 27 28
Day after Treatment 0 1 2 3 4 5 6 7
BAC treatment
Nifedipine/NPs treatment
Sacrifice
Body weight record
Fed food weight record
b
Body Weight of Individual Rat (g)
Healthy
Achalasia
Day 0
Day 7
Day 14
Day 21
Day after BAC Treatment (Modelling)
c
Healthy
Achalasia
d
Healthy
Sham
Saline
Free NFDP
NNPs
NFDP/NNPs
BNPs
NFDP/BNPs
Body Weight Increase of Individual Rat (g)
Day after Treatment
e
Intaked Food Weight of Individual Rat (g)
Day after Treatment

292

Figure 6. Achalasia model rats treated with free NFDP (nifedipine), saline, NNPs, BNPs, NFDP/NNPs, and NFDP/BNPs with comparison to healthy and sham-operated rats. a) Schematic detailing the 21-day development of the rat achalasia model following once daily treatment and monitoring over 7 days. b) Changes in the body weights of rats during the 21-day disease modeling period. c) X-ray images of esophageal tissues obtained from healthy rats and BAC-induced achalasia rats. d) Changes in the body weights of rats during the 7-day treatment period ($n = 5$ per group). e) Food intake of rats during the 7-day treatment period.

3. Conclusions

In this study we developed drug loaded BNPs for targeted treatment of esophageal disorders. BNPs were produced through oxidation of vicinal diols on the surface of PLA-HPG NPs, leading to exposure of aldehyde moieties on the NP surface that could bind to amine groups in amino acids. The bioadhesive properties of BNPs were confirmed using *in vitro*, *ex vivo*, and *in vivo* experiments, whereby the BNPs were demonstrated to adhere to poly-L-lysine plates, *ex vivo* human and rat esophageal tissue, and in *vivo* rat esophageal tissue significantly better than NNPs. Converting NNPs to BNPs, and subsequently loading BNPs with a model drug (NFDP) was found to have no effect on NP size or morphology. Moreover, drug-free and NFDP loaded BNPs were shown to have no cytotoxicity when applied to esophageal and intestinal cell lines at concentrations of ≤ 5 mg/mL. When administered to rats with simulated achalasia, BNPs were demonstrated to significantly enhance NFDP delivery to esophageal tissues whilst greatly limiting systemic drug exposure, compared to free NFDP and NFDP/NNPs. The safety of this site-specific drug delivery was demonstrated by a lack of gastric, intestinal, hepatic or splenic toxicity in rats administered the NFDP/BNPs. Finally, achalasia rats treated with NFDP/BNPs were observed to have significantly higher food intake and weight gain compared to those administered free NFDP, unloaded NPs, and NFDP/NNPs, demonstrating the novel formulation's superior

therapeutic efficacy. These results present BNPs as a promising formulation strategy for targeted drug delivery to the esophagus, providing opportunities for the development of new treatments aimed at improving the lives of patients suffering from esophageal conditions.

4. Materials and methods

Materials. Polylactic acid (Mw = 17.0 kDa) and $NaIO_4$ were from Shunna Biotechnology and Alalddin, respectively. Cy5 was obtained from Lumiprobe Corporation. Anhydrous dimethylformamide and dichloromethane were purchased from Innochem. Potassium methoxide, nifedipine (NFDP) and 1,1,1-trihydroxymethyl propan were supplied by Sigma-Aldrich. Anhydrous dry ether and Na_2SO_3 were obtained from Guangzhou Chemical Reagent Factory. All other chemicals are noted individually in the following methods.

Synthesis of HPG. 4.67 mmol 1,1,1-trihydroxypropane (THP) was added into an argon protected flask in a 95°C oil bath. When it was completely dissolved, 1.4 mmol $KOCH_3$ was added. The flask was connected to a vacuum pump for 10 min and then argon was filled in the flask all the time. 25 mL glycidol was added by a syringe pump 12.5 h. The HPG was dissolved in methanol and was precipitated with acetone. The HPG was purified by repeating this process three times. The HPG was dialyzed against DI water to get rid of small molecular weights of HPG. The water was replaced two times every 5 h. Acetone was added to precipitate the HPG and then the HPG was dried under vacuum at 85°C for 8 – 10 h.

Synthesis of PLA-HPG and PLA-Cy5 copolymers. 5 g PLA dissolved in DCM, and 2.3 g HPG dissolved in DMF was then added. They formulations were dried by molecular sieving for as long as possible. 0.08 mL diisopropylcarboimide (DIC) and 13.5 mg 4-(N,N-dimethylamino)pyridine (DMAP) was added and the reaction worked for 5 days at room temperature under stirring. Cold ether was added into the reaction

and the product was precipitated. The precipitate was collected by centrifugation. The product was re-dissolved in DCM and the subsequent product was precipitated with cold ether. The product was then dried under vacuum for 2 days. To synthesize PLA-Cy5, 1.95 g PLA dissolved in DCM, before the addition of 15 mg Cy5 and 0.02 mL diisopropylcarboimide (DIC). The reaction was subjected to stirring for one day at room temperature. Cold ether was added into the reaction and the product precipitated. which was collected by centrifugation. The product was dried under vacuum for 2 days.

Preparation of nanoparticles. The preparation of NNPs was conducted with 22.5 mg PLA-HPG copolymer dissolved in a mixture of 0.5 mL ethyl acetate and 0.35 mL DMSO. For the dye loaded and drug loaded nanoparticles preparation, 2.5 mg Cy5-PLA or NFDP was added into the PLA-HPG solution, respectively. The above mixture was added to 2 mL DI water under vortexing and subjected to probe sonication for three cycles at 10 s each. Subsequently, this emulsion was diluted with 10 mL DI water under stirring, and then transferred to a rotary evaporator to evaporate the ethyl acetate. The NNPs loaded with/without Cy5 or NFDP were obtained by centrifugation with Amico ultra-centrifuge filtration unit (100 k molecular weight cut-off (MWCO)) at a low temperature once and washed twice with DI water.

BNPs were obtained by $NaIO_4$ treatment of related NNPs. Briefly, one volume of NNPs was incubated with the same volume of $NaIO_4$ at 0.1 M for 2 min, and the reaction was subsequently quenched with one volume of Na_2SO_3 at 0.2 M. If the volume of NNPs was larger, three volume of $NaIO_4$ or Na_2SO_3, and longer reaction time would be needed. The BNPs loaded with/without Cy5 or NFDP were centrifuged at a low temperature once and washed twice with DI water. The nanoparticles were kept by being resuspended in DI water.

Characterization of nanoparticles. The diameter and polydispersity index (PDI) of nanoparticles were determined using a Zetasizer Nano ZS (Malvern Instruments). Particle morphologies were measured by transmission electron microscopy (TEM, Tecnai G2 Spirit, FEI). In a particular, a drop of NPs suspension was applied onto the carbon-supported copper grid, and another droplet of uranyl acetate was added

following. Most of the liquid drops were removed by a filter paper and wait for 5-10 min until it dries. The grid was transferred in a TEM holder and inserted into the microscope.

The *in vitro* concentration of Cy5 and NFDP was quantified with a plate reader by fluorescence (excitation wavelength: 650 nm; emission wavelength: 680 nm) and an absorption wavelength at 340 nm, respectively.

Cytotoxicity of nanoparticles. The cytotoxicity of NNPs, BNPs NFDP/NNPs and NFDP/BNPs was conducted in both epithelial cells from the human esophagus (Het-1A) and human colorectal adenocarcinoma cell (Caco-2). Het-1A (ATCC CRL-2692) and Caco-2 (ATCC HTB-37) were cultured in Bronchial Epithelial Cell Growth (BEG) medium (LONZA) and Dulbecco's modified eagle (DME) medium (GIBCO) supplemented with 10% fetal bovine serum and 1% penicillin/streptomycin, respectively.

Het-1A and Caco-2 in 100 μL of culture medium were plated in each well of a 96-well plate at a density of 5,000 and 10,000 cells per well, respectively. Cells in medium were maintained at 37°C to incubate overnight. The following day, 10 μL of either blank culture medium, NNPs, BNPs, NFDP/NNPs, NFDP/BNPs, was added to cells. Cells were incubated at 37°C for 24 h, and then cell viability was quantified with a Cell Counting Kit-8 (Dojindo).

Evaluation of NNPs and BNPs adhesion and permeation *ex vivo*. Fresh esophagus from human was obtained from who underwent surgery for esophageal cancer at the Third Affiliated Hospital of Sun Yat-sen University (Guangzhou, China). The experimental protocol (No. [2021]5-20) was approved by The Research Ethics Committee of the Third Affiliated Hospital of Sun Yat-sen University. All patients signed an informed consent form. The animal procedures were approved by The Animal Research Ethics Committee of Sun Yat-sen University. The esophagus of rats was collected immediately after sacrifice.

Esophageal tissues were placed on the petri dish as a sheet and washed with PBS. PLA-Cy5-loaded BNPs and NNPs in PBS were applied to the mucosal surface of esophagus,

and subsequently rinsed with PBS or simulated gastric fluid (pH 2.1). The nanoparticles remaining on the surface of esophageal tissues were imaged by Xenogen. These tissues were incubated for 1 h in a chamber at 37 °C with a humidity of 75%. Each esophagus was frozen in OCT, and sectioned into 10 μm slices, mounted on glass slides. The slices were imaged using an EVOS fluorescence microscope (Thermo Fisher).

Determination of NNPs and BNPs initial adhesion *in vivo.* All animal procedures were performed in accordance with Ruiye Model Animal (Guangzhou) Biotechnology protocols. Animals were kept in Ruiye Model Animal (Guangzhou) Biotechnology Co. Ltd. The Sprague-Dawley (SD) rats were housed at room temperature (25°C) and in a light-dark cycle of 12 h. To determine the NNPs and BNPs initial adhesion on esophagus, 2 mg/mL Cy5-NNPs or Cy5-BNPs in PBS was intraesophageally administrated to the rats. The rats were sacrificed immediately after the treatment, their esophagus was rapidly removed and frozen in OCT. The frozen tissue was sectioned into 10 μm slices and imaged using an EVOS fluorescence microscope.

Retention of NNPs and BNPs on esophagus *in vivo*. For evaluation of nanoparticles retention and distribution, 2 mg/mL Cy5-NNPs or Cy5-BNPs in PBS was intraesophageally administrated to the rats. After a series of time points, the rats were sacrificed with a CO_2 euthanasia chamber and the esophagus was rapidly removed. The nanoparticles remaining on the esophagus were imaged by Xenogen. All the rats were caged in groups of two, allowed to move freely and provided with food and water during the experiment.

Preparation of esophageal achalasia animal model. Male SD rats weighing around 300 g were anaesthetized with 4% chloral hydrate. An abdominal mid-line incision was made to expose the distal esophagus and proximal stomach. Benzyldimethyltetradecylammonium chloride (BAC) at 4 mM concentration was circumferentially injected with 100 μL of solution into the outer wall of 4 – 5 cm of the distal esophagus and 1 cm of the gastric cardia. The abdominal incision was closed in three layers with 3-0 chromic gut and 3-0 silk. The rats in the sham group underwent a similar surgery where 100 μL saline was injected into the lower esophagus and proximal

stomach.

21 days following surgery, BAC-treated animals and sham rats were anesthetized and underwent barium esophagrams. 1.0 mL barium contrast (50%) was orally administrated to each rat under fluoroscopy, and representative radiographs were obtained on each animal. The body weight of each rat was recorded every seven days during this period.

Retention profile of NFDP in esophageal tissue and plasma. 1 mL NFDP, NFDP/NNPs and NFDP/BNPs at the concentration of 2 mg/mL was delivered intra-esophageally. Subsequently, the achalasia rats were sacrificed after 0.1 h, 1 h, 2 h, 4 h, 6 h, 10 h and 24 h. Their esophageal tissues and blood were immediately excised and taken by cardiac puncture, respectively. Esophageal tissues were cut into small pieces and homogenized in 1 mL of PBS at 30 Hz for 180 s with TissueLyser II (QIAGEN). The blood samples were centrifuged at 10,000 rpm for 10 min, and 100 μL plasma (supernatant) was subsequently collected.

To quantify the NFDP in the biologic samples, 10 μL 1 mol/L NaOH and 0.6 mL ether-chloroform (5:1) were added into the tissue homogenized mixture and blood plasma, and centrifuged at 10,000 rpm for 10 min. The organic phase (supernatant) was subsequently collected and evaporated with a Speedvac (Yatai, Jilin, China). The dried residue was then dissolved in 0.2 mL of acetonitrile. An aliquot of 20 μL of each filtered sample was then processed on the LC-MS apparatus. The above operations were conducted in the condition of darkness.

Chromatographic analysis of NFDP in biologic samples. Chromatographic analysis was performed with a LC-MS system (Shimadzu LCMS-8060) equipped with pump (Shimadzu LC-30AD), autosampler (Shimadzu SIL-30AC) and a mass detector (Shimadzu LCMS-8060). The triple quadrupole mass spectrometer equipped with the positive electrospray ionization using multiple reaction monitoring (MRM) mode. Further instrumental conditions were 300°C source temperature, 250°C DL temperature, 10 L/min sheath gas flow, 10L/min drying gas flow, cone voltage 4.0 KV and 35 collision energy.

NFDP in the biological samples was determined by LC-MS with a C18 (2.1 mm × 100 mm, I.D./1.7 μm) analytical column (Waters). The mobile phases were 0.1 % formic acid in water and acetonitrile with a flow rate of 0.4 mL/min. The gradient elution procedure started with 30% acetonitrile, increasing to 80% over 10 min and then decreasing back to 30%. On the basis of the full-scan mass spectra, the most abundant ions and the product ions were selected: m/z 347.20 → 253.15.

Therapeutic efficacy of NFDP/BNPs *in vivo*. 1 mL of either PBS, NNPs, BNPs, NFDP, NFDP/NNPs or NFDP/BNPs at the dose of 2 mg/mL were intra-esophageally administrated to the esophageal achalasia rats (n = 6) daily. During the seven-days period, the body weight and up-take food volume of each rat were recorded.

Long-term toxicity of NFDP/BNPs *in vivo*. 1 mL of either PBS, NNPs, BNPs, NFDP, NFDP/NNPs or NFDP/BNPs at 2 mg/mL were administrated intraesophageally to achalasia rats daily. Seven days later, rats (n = 6) were sacrificed with a CO_2 euthanasia chamber, and their upper esophagus, stomach, intestine, liver and spleen were harvested for histological examination. Samples were fixed overnight in 10% formalin at room temperature and cut into sections. The tissue sections were dewaxed and debenzylated, followed by counterstaining with haematoxylin. Images for representative hematoxylin and eosin (H&E) staining tissue sections were collected using an Olympus BX61 microscope with a SPOT Flex 64 MP digital color camera.

Statistical analysis. The data are presented as the mean ± S.D. and statistical comparison of mean values were analyzed with Prism software (GraphPad) using ANOVA with multiple t-tests. Error bars represent standard deviation and have been indicated appropriately in each figure caption. All the experiments were carried out at least in triplicate. Significance is represented on plots as ns > 0.05, *< 0.05, ** < 0.01, ***< 0.001.

Acknowledgements

This work was supported by the National Natural Science Foundation of China [grant

numbers 82003672, 82104079]; and the Shenzhen Science and Technology Program [grant number KQTD20190929173853397, JCYJ20210324124602005].

Credit Author Statement

Yang Mai: Conceptualization, Methodology, Investigation, Data Curation, Writing - Original Draft, Visualization. **Yaqi Ouyang:** Methodology, Investigation, Data Curation, Visualization. **Yujia Qin:** Methodology, Investigation. **Changchang Jia:** Resources, Investigation. **Laura E. McCoubrey:** Writing - Review & Editing. **Abdul W. Basit:** Writing - Review & Editing. **Yichu Nie:** Resources. **Yizhen Jia:** Investigation. **Liu Yu:** Investigation. **Liu Dou:** Investigation. **Wenbin Deng:** Funding acquisition. **Yang Deng:** Conceptualization, Methodology, Supervision, Project administration, Funding acquisition. **Yang Liu:** Conceptualization, Methodology, Writing - Review & Editing, Supervision, Project administration.

Declaration of Competing Interest

Authors declare that they have no competing interests.

Data and materials availability

All data are available in the main text or the supplementary materials.

References

[1] National Cancer Institute, Cancer Stat Facts: Esophageal Cancer, 2021. https://seer.cancer.gov/statfacts/html/esoph.html. Accessed 4 March 2022.

[2] Y.-M. Yang, P. Hong, W.W. Xu, Q.-Y. He, B. Li, Advances in targeted therapy for esophageal cancer, Signal Transduct Target Ther 5 (2020) 229.

[3] C.E. Gaber, S. Eluri, C.C. Cotton, P.D. Strassle, T.M. Farrell, J.L. Lund, E.S. Dellon, Epidemiologic and Economic Burden of Achalasia in the United States, Clin Gastroenterol H 20 (2021) 342-352.

[4] T. Yamasaki, C. Hemond, M. Eisa, S. Ganocy, R. Fass, The Changing Epidemiology of

514 Gastroesophageal Reflux Disease: Are Patients Getting Younger?, J Neurogastroenterol 24
515 (2018) 559-569.
516 [5] N.J. Shaheen, V. Mukkada, C.S. Eichinger, H. Schofield, L. Todorova, G.W. Falk, Natural
517 history of eosinophilic esophagitis: a systematic review of epidemiology and disease course,
518 Dis Esophagus 31 (2018) 1-14.
519 [6] H. Batchelor, Bioadhesive Dosage Forms for Esophageal Drug Delivery, Pharm Res-Dordr
520 22 (2005) 175-181.
521 [7] Y.A. Aly, H. Abdel-Aty, Normal oesophageal transit time on digital radiography, Clin Radiol
522 54 (1999) 545-549.
523 [8] F. Taherali, F. Varum, A.W. Basit, A slippery slope: On the origin, role and physiology of
524 mucus, Adv Drug Deliver Rev 124 (2018) 16-33.
525 [9] S. Kobayashi, N. Kanai, T. Ohki, R. Takagi, N. Yamaguchi, H. Isomoto, Y. Kasai, T. Hosoi,
526 K. Nakao, S. Eguchi, M. Yamamoto, M. Yamato, T. Okano, Prevention of esophageal strictures
527 after endoscopic submucosal dissection, World J Gastroentero 20 (2014) 15098-15109.
528 [10] G.S. McCord, R.E. Clouse, Pill-induced esophageal strictures: clinical features and risk
529 factors for development, Am J Med 88 (1990) 512-518.
530 [11] A.C. Perkins, C.G. Wilson, M. Frier, P.E. Blackshaw, R.J. Dansereau, R.M. Vincent, D.
531 Wenderoth, S. Hathaway, Z. Li, R.C. Spiller, The use of scintigraphy to demonstrate the rapid
532 esophageal transit of the oval film-coated placebo risedronate tablet compared to a round
533 uncoated placebo tablet when administered with minimal volumes of water, Int J Pharm 222
534 (2001) 295-303.
535 [12] M. Lin, N. Firoozi, C.T. Tsai, M.B. Wallace, Y. Kang, 3D-printed flexible polymer stents
536 for potential applications in inoperable esophageal malignancies, Acta Biomater 83 (2019) 119-
537 129.
538 [13] J. Chen, L. Zhou, C. Wang, Y. Sun, Y. Lu, R. Li, X. Hu, M. Chen, L. Chen, K. Chai, T. Yao,
539 S. Shi, C. Dong, A multifunctional SN38-conjugated nanosystem for defeating
540 myelosuppression and diarrhea induced by irinotecan in esophageal cancer, Nanoscale 12(41)
541 (2020) 21234-21247.
542 [14] E. Coffin, A. Grangier, G. Perrod, M. Piffoux, I. Marangon, I. Boucenna, A. Berger, L.
543 M'Harzi, J. Assouline, T. Lecomte, A. Chipont, C. Guerin, F. Gazeau, C. Wilhelm, C. Cellier,
544 O. Clement, A.K.A. Silva, G. Rahmi, Extracellular vesicles from adipose stromal cells
545 combined with a thermoresponsive hydrogel prevent esophageal stricture after extensive
546 endoscopic submucosal dissection in a porcine model, Nanoscale 13(35) (2021) 14866-14878.
547 [15] P. Didden, M.C.W. Spaander, M.J. Bruno, E.J. Kuipers, Esophageal Stents in Malignant
548 and Benign Disorders, Curr Gastroenterol Rep 15 (2013) 319.
549 [16] J. Krause, C. Rosenbaum, M. Grimm, A. Rump, R. Kessler, N. Hosten, W. Weitschies, The
550 EsoCap-system - An innovative platform to drug targeting in the esophagus, J Control Release
551 327 (2020) 1-7.
552 [17] L. Zhang, D. Russell, B.R. Conway, H. Batchelor, Strategies and therapeutic opportunities

for the delivery of drugs to the esophagus, Critl Rev Ther Drug 25 (2008) 259-304.
[18] J.D. Naranjo, L.T. Saldin, E. Sobieski, L.M. Quijano, R.C. Hill, P.G. Chan, C. Torres, J.L. Dziki, M.C. Cramer, Y.C. Lee, R. Das, A.K. Bajwa, R. Nossair, M. Klimak, L. Marchal, S. Patel, S.S. Velankar, K.C. Hansen, K. McGrath, S.F. Badylak, Esophageal extracellular matrix hydrogel mitigates metaplastic change in a dog model of Barrett's esophagus, Sci Adv 6(27) (2020) eaba4526.
[19] I. Djordjevic, O. Pokholenko, A.H. Shah, G. Wicaksono, L. Blancafort, J.V. Hanna, S.J. Page, H.S. Nanda, C.B. Ong, S.R. Chung, A.Y.H. Chin, D. McGrouther, M.M. Choudhury, F. Li, J.S. Teo, L.S. Lee, T.W.J. Steele, CaproGlu: Multifunctional tissue adhesive platform, Biomaterials 260 (2020) 120215.
[20] H.K. Batchelor, D. Banning, P.W. Dettmar, F.C. Hampson, I.G. Jolliffe, D.Q.M. Craig, An *in vitro* mucosal model for prediction of the bioadhesion of alginate solutions to the oesophagus, Int J Pharm 238 (2002) 123-132.
[21] S. Collaud, T. Warloe, O. Jordan, R. Gurny, N. Lange, Clinical evaluation of bioadhesive hydrogels for topical delivery of hexylaminolevulinate to Barrett's esophagus, J Control Release 123 (2007) 203-210.
[22] M. Säkkinen, J. Marvola, H. Kanerva, K. Lindevall, A. Ahonen, M. Marvola, Scintigraphic verification of adherence of a chitosan formulation to the human oesophagus, Eur J Pharm Biopharm 57 (2004) 145-147.
[23] Y. Deng, J.K. Saucier-Sawyer, C.J. Hoimes, J. Zhang, Y.E. Seo, J.W. Andrejecsk, W.M. Saltzman, The effect of hyperbranched polyglycerol coatings on drug delivery using degradable polymer nanoparticles, Biomaterials 35 (2014) 6595-6602.
[24] S. Liu, S.H. Qin, M. He, D.F. Zhou, Q.D. Qin, H. Wang, Current applications of poly(lactic acid) composites in tissue engineering and drug delivery, Compos Part B-Eng 199 (2020) 108238.
[25] R. Guo, K.K. Li, J. Qin, S.L. Niu, W. Hong, Development of polycationic micelles as an efficient delivery system of antibiotics for overcoming the biological barriers to reverse multidrug resistance in Escherichia coli (vol 17, pg 531, 2020), Nanoscale 12(22) (2020) 12172-12172.
[26] Y. Deng, A. Ediriwickrema, F. Yang, J. Lewis, M. Girardi, W.M. Saltzman, A sunblock based on bioadhesive nanoparticles, Nat Mater 14 (2015) 1278-1285.
[27] Y. Deng, F. Yang, E. Cocco, E. Song, J. Zhang, J. Cui, M. Mohideen, S. Bellone, A.D. Santin, W.M. Saltzman, Improved i.p. drug delivery with bioadhesive nanoparticles, P NatAcad Sci 113 (2016) 11453-11458.
[28] J.K. Hu, H.-W. Suh, M. Qureshi, J.M. Lewis, S. Yaqoob, Z.M. Moscato, S. Griff, A.K. Lee, E.S. Yin, W.M. Saltzman, M. Girardi, Nonsurgical treatment of skin cancer with local delivery of bioadhesive nanoparticles, P Nat Acad of Sci USA 118 (2021) e2020575118.
[29] A. Nassri, Z. Ramzan, Pharmacotherapy for the management of achalasia: Current status, challenges and future directions, World J Gastrointest Pharmacol Ther 6 (2015) 145-155.

592 [30] A. Banerjee, J.P. Qi, R. Gogoi, J. Wong, S. Mitragotri, Role of nanoparticle size, shape and
593 surface chemistry in oral drug delivery, J Control Release 238 (2016) 176-185.
594 [31] S. Bredenberg, C. Nystrom, In-vitro evaluation of bioadhesion in particulate systems and
595 possible improvement using interactive mixtures, J Pharm Pharmacol 55(2) (2003) 169-77.
596 [32] J.W. Kikendall, M.H. Mellow, Effect of sublingual nitroglycerin and long-acting nitrate
597 preparations on esophageal motility, Gastroenterology 79 (1980) 703-706.
598 [33] A.G. Sabirov, I.S. Raginov, M.V. Burmistrov, Y.A. Chelyshev, R. Khasanov, A.A.
599 Moroshek, P.N. Grigoriev, A.L. Zefirov, M.A. Mukhamedyarov, Morphofunctional analysis of
600 experimental model of esophageal achalasia in rats, B Exp Biol Med 149 (2010) 466-470.